

Sub-20-ps pulses from a passively Q-switched microchip laser at 1 MHz repetition rate

Eva Mehner,^{1,2,*} Benjamin Bernard,¹ Harald Giessen,² Daniel Kopf,³ and Bernd Braun¹

¹Nuremberg Institute of Technology Georg Simon Ohm, Keßlerplatz 12, 90489 Nuremberg, Germany

²4th Physics Institute and Research Center SCoPE, University of Stuttgart, Pfaffenwaldring 57, 70550 Stuttgart, Germany

³Montfort Laser GmbH, Im Holderlob 6a, A-6840 Götzis, Austria

*Corresponding author: eva.mehner@th-nuernberg.de

Received February 19, 2014; revised April 3, 2014; accepted April 13, 2014;

posted April 14, 2014 (Doc. ID 205829); published May 9, 2014

We present a 50 μm $\text{Nd}^{3+}:\text{YVO}_4$ microchip laser that is passively Q-switched by a semiconductor saturable absorber mirror. To reduce handling problems caused by the small crystal dimensions, the 50 μm $\text{Nd}^{3+}:\text{YVO}_4$ crystal is optically bonded to an undoped YVO_4 crystal of a length of about 500 μm . By using a saturable absorber mirror with an effective modulation depth of $>10\%$ the system is able to deliver 16 ps pulses at a repetition rate of up to 1.0 MHz. The average laser power is 16 mW at 1064 nm. To our knowledge these are the shortest Q-switched pulses ever reported from a solid-state laser. The limits in terms of pulse width, repetition rate, output power, and system stability are discussed. Additionally, continuous-wave behavior is analyzed. Experimental data is compared with the simulation results of the coupled rate equations. © 2014 Optical Society of America

OCIS codes: (140.3530) Lasers, neodymium; (140.3540) Lasers, Q-switched.

<http://dx.doi.org/10.1364/OL.39.002940>

Within the last decade short-pulse laser systems have found entry into industrial micromaterial fabrication processes on a large scale. Equally, the demand of simple, compact, and cost-effective seed sources has grown enormously. For these applications pulse durations in the range of a few hundred femtoseconds to some 10 ps at repetition rates in the range between 1 and 5 MHz are required. Up to now, mode locked laser oscillators were used to achieve the ultrashort pulse widths [1]. However, the repetition rates of these systems are too high, whereas the pulse energies are too low. Therefore, a subsequent pulse picker and amplifier stage are necessary. Unfortunately these systems are rather complex and expensive. Alternatively, long resonators with Herriott-type multipass cells [2,3] and cavity dumped systems were demonstrated [4].

In comparison it is strikingly simple to use Q-switched microchip lasers and a subsequent single-pass amplifier instead [5–12]. The main benefits of these microchip lasers are their small size and potentially straightforward fabrication process which enables them to become a low-cost mass product. Microchip lasers are solid-state lasers with a quasi-monolithic setup. The solid-state gain material is polished flat and parallel on both sides. The laser crystal itself forms the resonator. Due to the short cavity length, the cavity mode spacing is usually greater than the gain bandwidth, which allows single longitudinal mode operation. Additionally a diffraction limited output beam can be achieved by properly controlling the thermally induced lens and matching the laser mode size to the pump mode size [13]. Most importantly, the cavity length is directly proportional to the pulse width if a saturable absorber such as $\text{Cr}^{4+}:\text{YAG}$ [7] or a semiconductor saturable absorber mirror (SESAM) [14] is used for passive Q-switching. This allows Q-switched pulses well below 100 ps [8,9,15,16]—a parameter range which was accessible in the past only by mode-locked laser oscillators.

In this Letter, we will present a 50 μm $\text{Nd}^{3+}:\text{YVO}_4$ microchip laser that is passively Q-switched by a SESAM.

After discussing the theory of operation the experimental results in continuous-wave and pulsed laser operation for different SESAMs are shown, discussed, and compared with theoretical calculations.

To attain the desired short pulses the setup parameters have to be designed carefully. Using Eq. (1) a rough estimate for the pulse duration can be carried out [8,16,17]:

$$\tau_{\text{pulse}} = \frac{3.52 \cdot T_R}{q_0}. \quad (1)$$

The key parameters are the cavity round trip time T_R and the loss coefficient of the absorber q_0 (please note that sometimes the value of 3.52 is approximated by a value of 4 and the loss and gain coefficients are given with respect to the amplitude rather than the intensity, which accounts for a factor of 2). For shortest pulses a high modulation depth, that is, a large loss coefficient and a short cavity length, is required.

Butler *et al.* predicted a minimum cavity length for stable Q-switched laser operation depending on different system parameters [15]. They examined the influence of an etalon, namely the thickness of the air layer between the absorber and the crystal. This etalon has an important influence on the effective modulation depth of the absorber, as was also discussed in [13]. They achieved a pulse width of about 22 ps with a 110 μm thick $\text{Nd}^{3+}:\text{YVO}_4$ crystal. The modulation depth was about 23% in the case of a resonant etalon. In addition they discussed the problem of two-photon absorption (TPA) within the absorber, which is a source of perturbation when considering the complete bleaching of the saturable absorber. They also mentioned that TPA has little effect on pulse duration; it is therefore neglected in our calculations [15].

With Eq. (1) for a 50 μm long crystal, one would expect pulse durations between 15 and 60 ps for modulation depths of the SESAM between 20% and 5% (Table 1). In comparison the pulse widths are given in parentheses

Table 1. Theoretically Achievable Pulse Duration for a 50 μm Cavity

Modulation Depth (%)	τ_{pulse} (ps)
5	51 (59)
10	25 (31)
20	13 (16)

as they result from a numerical integration of the rate equations [16,17].

A theoretical estimate for the maximum extractable pulse energy can be calculated by [16,17]:

$$E_p = \frac{h\nu_L}{2\sigma_L} A 2q_0 \frac{l_{\text{out}}}{l_{\text{out}} + l_p}, \quad (2)$$

for $q_0 \leq l = l_{\text{out}} + l_p$. $e_L = (h\nu_L/2\sigma_L)$ is the saturation fluence of the gain material, A is the mode area within the gain material, l_{out} is the output coupling coefficient, q_0 is the loss coefficient of the absorber, and l_p is the parasitic nonsaturable loss coefficient of the system [16,17], all with respect to the intensity.

Our setup is displayed in Fig. 1. A fiber coupled laser diode (LD) from Bright Solutions SRL, Cura Carpignano (Pavia), Italy, is used as pump source. The LD delivers up to 12 W of optical power at a wavelength of 808 nm (fiber core diameter: 100 μm , NA = 0.18). The pump radiation is collimated and focused by a pair of focusing lenses with focal lengths of $f = 35$ mm and $f = 18$ mm (aspheric lens). Thus, a pump spot diameter of about 54 μm is achieved. Such a small pump spot diameter is necessary to obtain high pump intensities. These are important to overcome the high losses of the system, which result from the required high modulation depth of the absorber for the generation of short pulses, as discussed earlier.

A dichroic beam splitter (DBS) is used for separation of the pump and the laser radiation. This dichroic mirror is antireflective coated for the pump wavelength at 808 nm and high reflective for the laser wavelength at 1064 nm.

Because of its high absorption coefficient of 31.4 cm^{-1} [18] and its high emission cross section parallel to the c axis of about $25 \times 10^{-19} \text{ cm}^2$ [18], an a -cut $\text{Nd}^{3+}:\text{YVO}_4$ is used as the laser active material. The doping is 3 at. %. To overcome the physical limitations, when shrinking the crystal size, an optically bonded crystal setup was used for the microchip laser. The 50 μm $\text{Nd}^{3+}:\text{YVO}_4$ crystal we

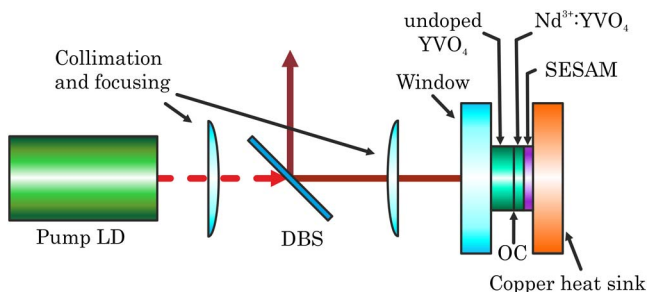


Fig. 1. Experimental setup: passively Q -switched microchip laser pumped by a 808 nm LD with a DBS for separation of pump and laser radiation.

used is bonded to an undoped YVO_4 crystal with a thickness of about 500 μm . The optical coating for the output coupling (OC) is located at the interface of the two crystals. The transmission for the laser wavelength at 1064 nm is chosen to be 5%. The second end mirror is formed by a SESAM [14]. To sandwich this bonded crystal system an additional window is used. It has an antireflective coating on both sides for the pump and the laser wavelength.

The SESAMs we tested have recovery times in the range of 100 ps to 1 ns. The fluence is estimated to be approximately $120 \mu\text{J}/\text{cm}^2$. The modulation depth is varied between of 5% and 20%. The SESAMs were high-reflection coated with respect to the pump wavelength to prevent presaturation of the SESAMs by the pump light and to obtain a double-pass absorption of the pump light.

A crucial point concerning the laser operation is the parallelism of the end faces of the resonator. Therefore an excellent “sandwiching” of the components is essential.

First we performed continuous-wave measurements with a Bragg reflector instead of the SESAM. The results are displayed in Fig. 2.

Despite the short crystal length it was possible to achieve an optical output power of up to 100 mW at a pump power of 1.25 W. The optical-to-optical slope efficiency for continuous-wave operation is about 9% with respect to the incident pump power. With the absorption coefficient of 31.4 cm^{-1} [18] we estimate the amount of absorbed pump power to be 25%–30%. In the following all values for the pump power and the efficiencies are given with respect to the incident light.

Furthermore, the experimental results of the pulsed laser operation for two absorbers are shown in Figs. 3 and 4. They show the average output power, the repetition rate, and the pulse duration as a function of the optical pump power.

The pulse duration was measured with a “pulseCheck USB” autocorrelator by APE Angewandte Physik und Elektronik GmbH, Berlin. A fast photodiode from ALPHALAS GmbH, Göttingen, was used to measure the repetition rate (UPD40-VSI-P, 8.5 GHz bandwidth, 40 ps rise time).

As expected, by increasing the pump power the average output power and the repetition rate increase linearly

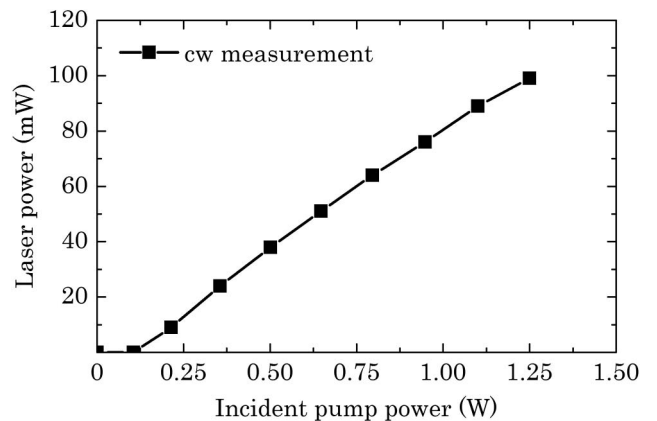


Fig. 2. Continuous-wave operation of the microchip laser: laser power as a function of incident pump power.

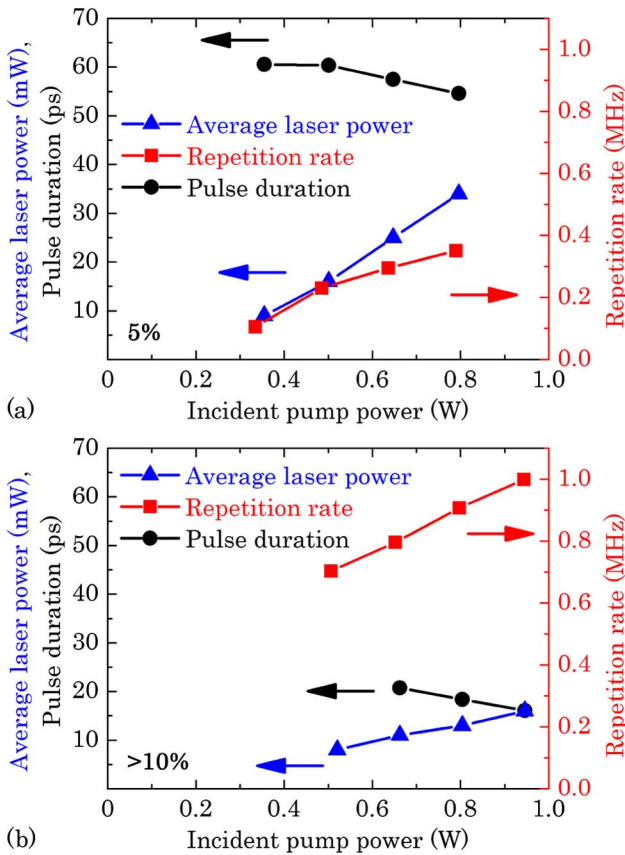


Fig. 3. Pulsed laser operation of the microchip laser for the SESAMs with (a) 5% and (b) >10% modulation depth: average laser power (triangles), repetition rate (squares), and pulse duration (circles) as a function of incident pump power.

with the pump power, while the pulse energy as well as the pulse duration stay nearly constant [16]. An increase of the modulation depth results in a reduction of the pulse duration, as can be seen in Fig. 3. This agrees well with the prediction of Eq. (1).

We achieved 34 mW average output power at up to a 0.35 MHz repetition rate by using the SESAM with 5% modulation depth. The average pulse energy is around 85 nJ. The pulse duration was measured to be around 58 ps. For the SESAM with >10% modulation depth, up to 16 mW average output power at up to 1.0 MHz repetition rate was obtained. The pulse duration varied between 16 and 21 ps, assuming a sech^2 pulse shape and a deconvolution factor of 0.648 (and between 18 and 23 ps assuming a Gaussian pulse shape and a deconvolution factor of $1/\sqrt{2}$). The average pulse energy is around 14 nJ, which results in a fluence of about 0.7 mJ/cm^2 . BATOP GmbH, Jena [19], specifies the damage threshold of their SESAMs to be around 2 mJ/cm^2 . Thus, the system still operates well below the damage threshold of the absorber.

The autocorrelation trace of a single pulse with a pulse width of 16 ps is shown in Fig. 4.

The beam quality was measured with a Spiricon “ $M^2 - 200$ ” to be between 3.5 and 4.5 within the pump range.

The theoretically achievable maximum extractable pulse energy was estimated for the setup with the 5% SESAM with Eq. (2). The nonsaturable losses consist

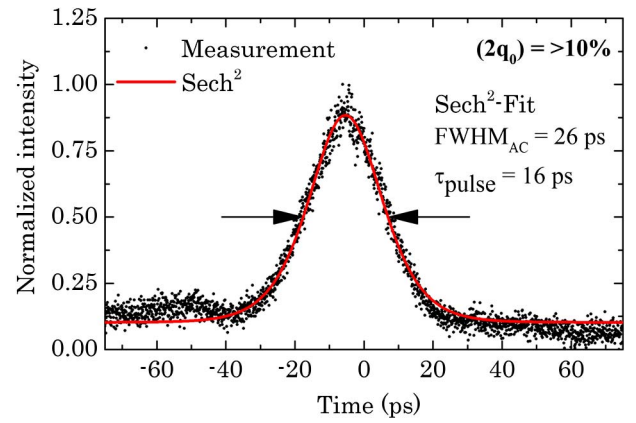


Fig. 4. Autocorrelation trace of a single pulse for the SESAM with >10% modulation depth.

of a 5% output coupler, nonsaturable losses of the SESAM between 2% and 3%, and additional parasitic losses which add to a total sum of nonsaturable losses between 7% and 10%. The extractable pulse energy is predicted to be about 50 nJ for the SESAM with 5% modulation depth. This compares fairly well with the measured value of 85 nJ.

Additionally, we compared our experimental measurement results with the simulation results of the coupled rate equations [16,17]. As an example, the results for the SESAM with 5% modulation depth are displayed in Fig. 5. The results fit quite well, though further losses exist within the system. For these calculations the total nonsaturable losses are assumed to be 10%. The effective modulation depth of the absorber within the simulation was assumed to be 4%, which indicates that the absorber is not completely bleached in practice. This results most likely from an air layer between the crystal and the SESAM which acts as an etalon, as already discussed in [13,15].

Furthermore, we compared the autocorrelation trace of the measured pulse to the autocorrelation of a simulated pulse. An example for a 16 ps pulse is displayed in Fig. 6.

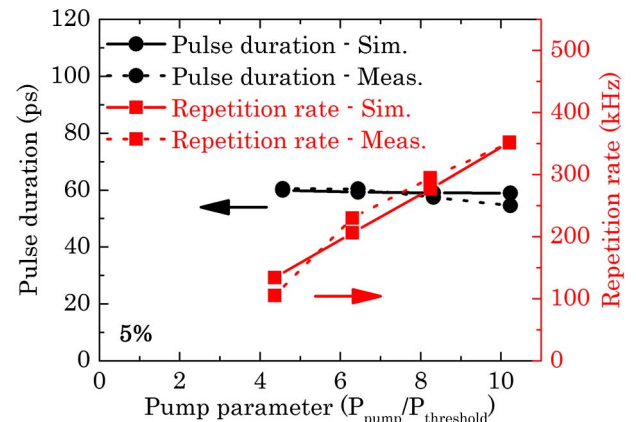


Fig. 5. Repetition rate (squares) and pulse duration (circles) as a function of the pump parameter (ratio of pump power to threshold power) for a SESAM with 5% modulation depth: comparison of measurement (dotted line) and simulation (solid line).

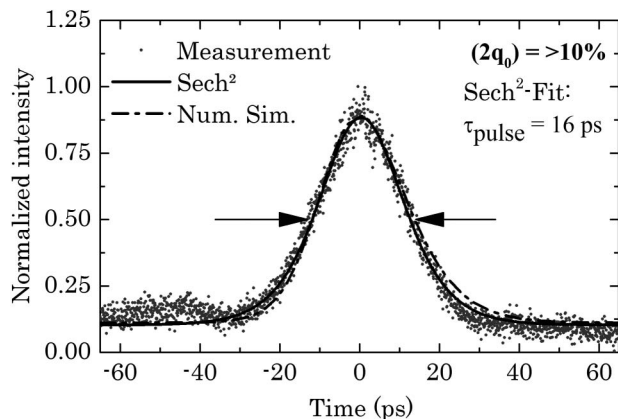


Fig. 6. Autocorrelation trace for a measured 16 ps pulse (gray dots), and sech^2 fit (solid line); comparison with autocorrelation function of simulated pulse (dashed dotted line) (deconvolution factor: 0.645).

As can be seen, the measured autocorrelation trace of a single pulse fits very well to its numerical result.

In conclusion, we presented a microchip laser that was passively Q -switched by a SESAM. The handling of the $50\ \mu\text{m}$ $\text{Nd}^{3+}:\text{YVO}_4$ crystal was made possible by bonding the crystal on a $500\ \mu\text{m}$ undoped YVO_4 crystal. An output power of up to 100 mW was attained in continuous-wave operation. Different SESAMs were tested. By using a SESAM with $>10\%$ modulation depth the system delivers 16 ps pulses at 1064 nm wavelength. The average output power was 16 mW at a repetition rate of 1.0 MHz. It is shown that the experimental results fit well to the simulation results of the coupled rate equations.

H. Giessen thanks Baden-Württemberg-Stiftung, BMBF, DFG, and ERC for funding.

References

1. C. Hönninger, R. Paschotta, M. Graf, F. Morier-Genoud, G. Zhang, M. Moser, S. Biswal, J. Nees, A. Braun, G. A. Mourou,

- I. Johannsen, A. Giesen, W. Seeber, and U. Keller, *Appl. Phys. B* **69**, 3 (1999).
2. A. Sennaroglu, A. M. Kowalewicz, E. P. Ippen, and J. G. Fujimoto, *IEEE J. Quantum Electron.* **40**, 519 (2004).
3. A. Sennaroglu and J. G. Fujimoto, *Opt. Express* **11**, 1106 (2003).
4. A. Killi, A. Steinmann, J. Dörring, and U. Morgner, *Opt. Lett.* **30**, 1891 (2005).
5. J. J. Zayhowski, *Opt. Lett.* **16**, 575 (1991).
6. J. J. Zayhowski, *Opt. Mater.* **11**, 255 (1999).
7. J. J. Zayhowski and C. Dill III, *Opt. Lett.* **19**, 1427 (1994).
8. B. Braun, F. X. Kärtner, G. Zhang, M. Moser, and U. Keller, *Opt. Lett.* **22**, 381 (1997).
9. D. Nodop, J. Limpert, R. Hohmuth, W. Richter, M. Guina, and A. Tünnermann, *Opt. Lett.* **32**, 2115 (2007).
10. A. Steinmetz, D. Nodop, J. Limpert, R. Hohmuth, W. Richter, and A. Tünnermann, *Appl. Phys. B* **97**, 317 (2009).
11. X. Délen, F. Balembois, and P. Georges, *J. Opt. Soc. Am. B* **29**, 2339 (2012).
12. A. Steinmetz, F. Jansen, F. Stutzki, R. Lehneis, J. Limpert, and A. Tünnermann, *Opt. Lett.* **37**, 2550 (2012).
13. E. Mehner, A. Steinmann, R. Hegenbarth, H. Giessen, and B. Braun, *Appl. Phys. B* **112**, 231 (2013).
14. U. Keller, K. J. Weingarten, F. J. Kärtner, D. Kopf, B. Braun, I. D. Jung, R. Fluck, C. Hönninger, N. Matuscheck, and J. Aus der Au, *IEEE J. Sel. Top. Quantum Electron.* **2**, 435 (1996).
15. A. C. Butler, D. J. Spence, and D. W. Coutts, *Appl. Phys. B* **109**, 81 (2012).
16. G. J. Spühler, R. Paschotta, R. Fluck, B. Braun, M. Moser, G. Zhang, E. Gini, and U. Keller, *J. Opt. Soc. Am. B* **16**, 376 (1999).
17. B. Braun, "Compact pulsed diode-pumped solid-state lasers," Ph.D. dissertation, No. 11953 (ETH, 1996).
18. CASTECH Inc., <http://www.optics.gwu-group.com/index.php/download/finish/3-castech-crystals/164-castech-laser-crystals-all.html>
19. BATOP GmbH, <http://www.batop.de/products/saturable-absorber/saturable-absorber-mirror/data-sheet/saturable-absorber-mirror-1064nm/saturable-absorber-mirror-SAM-1064-23-124ps.pdf>.